

Exoskeletal Spine and Shoulders for Full Body Exoskeletons in Health Care

Stefan Roland Taal* and Yoshiyuki Sankai

*Cybernetics Research Building, Graduate School of Systems and Information Engineering,
University of Tsukuba, 1-1-1 Tennodai, Tsukuba, Ibaraki, Japan*

ABSTRACT

Currently, full body exoskeletons still lack movability in their back and shoulder parts, resulting in limited applicability in, e.g., nursing care. An exoskeletal spine and shoulder mechanism called “exo-spine” has therefore been developed with the purpose of allowing 3 degree of freedom (DOF) spinal motion and 2 DOF shoulder girdle abduction. It consists of a mechanism of vertebrae, shoulder blades, and two cables for actuation such that only one motor is required. Control equations were obtained through measurements and friction analysis. Experiments were performed with a subject wearing the exo-spine in a simplified full body exoskeleton. The wearer was able to lift up to 40 kg using all DOF of the system. From this we confirmed the exo-spine’s 5 DOF movability and lifting performance. Next, the exo-spine will be installed in HAL exoskeletons in order to increase their usability in health care settings.

Keywords: Spine, exoskeleton, cable actuation, health care, lifting.

INTRODUCTION

With the aging of many advanced societies the work load for health care workers has already risen substantially. Despite all the interventions in health care work, such as [1] [2], it is still dangerous to the workers’ own health, resulting in many cases of back pain [3]. Patient handling techniques have been designed to prevent this [4], but at the same time they restrict the normal human adaptability to do a variety of tasks, i.e., they complicate the “control problem” [5] of, e.g., how to help a fallen patient up from the floor.

One type of solution developed recently that can increase the lifting ability of health care workers are full body exoskeletons [6] [7]. While they have shown promising results, they also decrease their wearer’s movability by restricting many of his normal degrees of freedom (DOF), mainly around the hips, back and shoulders, making it impossible to reach the floor to help up the patient. If exoskeletons could assist with lifting heavy loads using a larger variety of postures, including those that are normally unhealthy such as lifting with a flexed or twisted back [4], they would increase their wearer’s ability to solve each task’s control problem while still preventing

back pain. Much like a lifting team of several workers, one trained person wearing such a versatile exoskeleton would be able to provide the same lifting assistance.

Given the arrangement of DOF on the human body, full versatility in exoskeletons is especially difficult to achieve for the upper body. Full arm actuation for all DOF has been done, such as [8], although not yet in untethered, fully wearable types. Currently, the part of full body exoskeletons that is restricting the wearer's versatility the most is the part between the hips and shoulders, which is often completely rigid. Since altogether these parts contain 7 DOF, exoskeletons would require 7 extra actuators, using standard robotics technology, to regain this movability.

At present, several exoskeletal devices exist that assist (parts of) the shoulder and back. They can be grouped as follows. Exoskeletons with an unlimited power supply include both wearable types with a tether as well as those fixed to a base [8-10]. Although wearability is restricted to the power supply, this group has few limitations on the amount of actuators. Two solutions for shoulder motion can be seen: free shoulders and arms with interaction at the hands [7], and full actuation using one motor per DOF [8] [10]. Another group consists of full body exoskeletons that carry their own power supply [6] [7] [11]. With this extra limitation on the amount of actuators neither spine motion nor shoulder girdle motion has been implemented. Another group of more lightweight exoskeletal devices that attach to the arm are used for rehabilitation and force feedback systems [12] [13]. Their applications allow for a separate power supply and the required actuator forces are lower, such that full shoulder actuation is possible. Comparing the above devices it can be concluded that the available power imposes strong limitations on a battery powered, full body exoskeleton, especially for spinal movements. In addition, the conventional solution of one actuator per DOF would require more motors than can be carried along.



Figure 1 : Example setting of the HAL-5 robot suit for nursing care.

1.1 Setting and purpose

This research is part of the ongoing work with the robot suit HAL (Hybrid Assistive Limb) to develop a solution for nursing care (Fig. 1). The current HAL suit, HAL-5, is a full body exoskeleton that carries its own power supply [6]. It consists of frames interconnected by power units that each contain an electromotor and are positioned directly next to the hip, knee, shoulder (flexion) and elbow joints of the wearer. Additional passive DOF are located at each shoulder, upper arm, and ankle joint. The system is controlled according to the intentions of the wearer,

which are obtained by measuring the bioelectric signal (BES) on the skin above the main flexor and extensor muscles associated with each augmented human joint. Motor torques are calculated according to these signals. This “voluntary control” method as well as the actuators and electronics used in HAL-5 are also used in this research.

In order to solve the problems encountered with the spinal and shoulder flexibility of exoskeletons in health care work, this research’ purpose is to present a novel solution called “exo-spine” that provides the required flexibility and lifting assistance, i.e. 3 DOF spinal and 2 DOF shoulder girdle motion with augmentation for lifting in the front. Moreover, by maximizing the effectiveness of its actuation towards the achievement of heavy work it is able to do so using only one motor. More generally, the proposed solution will be important for exoskeletons in all kinds of settings, such as rescue work, factories and agriculture, increasing their applicability to a larger variety of tasks.

MATERIALS AND METHODS

This section will first describe the background and requirements for the exo-spine. After that the mechanics and control will be handled one by one. See [14] for a more extended discussion of some of the mechanical details shown here.

2.1 Exo-spine general design

In order to simplify the mechanism and its actuation it will be useful to look at the required support forces during usage. Rosen *et al.* found that when performing daily living tasks the gravitational component of the support forces accounts for more than 90% of the total forces [15]. In addition, during heavy lifting tasks gravity forces will account for almost all required actuation. Furthermore, the objects that are to be lifted are too heavy and large for the wearer to carry them on one side while still being able to walk in a balanced way. Therefore, the assistive forces the spine and shoulder girdle need are those that assist these parts to counter gravity forces from loads in the front. Instead of having as many actuators as the total number of DOF it would thus be more effective to use a few actuators that focus on such lifting action only.

With this, and the notion of the “neutral position” as the straight and non-rotated spine position, the purposes and design requirements of the different DOF are as follows:

- **Spine flexion (forward bending)**

Because lifting is in front this is the most important DOF. It extends the total flexion range of the upper body and allows for more natural bending postures. Due to the position behind the wearer the exo-spine is required to extend when flexing.

- **Spine lateral flexion (sideways bending, left or right)**

The purpose is to be able to lift up or put down objects that are tilted sideways; it is not meant to lift up objects from the side. The required forces are always toward the neutral position in order to balance the weight of the wearer and the load as their center of mass moves somewhat sideways.

- **Spine rotation (rotation around the vertical axis)**

Rotation can be used, for example, to move objects sideways or to extend the reach of one arm when reaching over a bed. To prevent large rotations when carrying heavy loads a supporting torque towards the neutral position should be included.

• Shoulder girdle motion

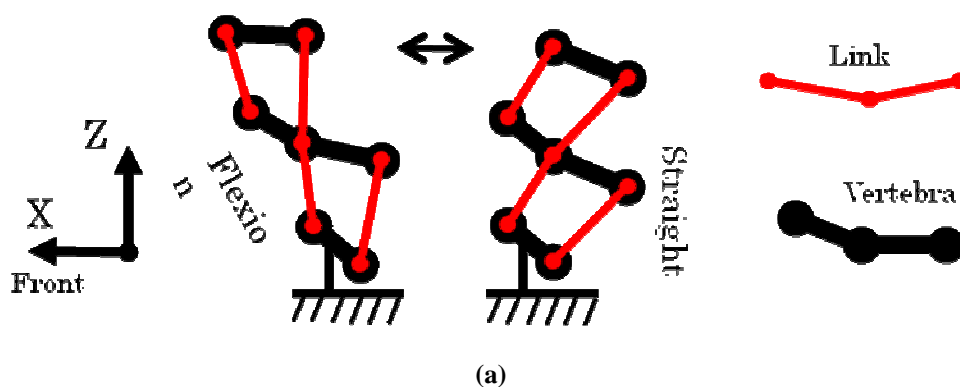
Its purpose is to allow deeper flexing of the upper body, meaning that especially abduction (forward motion) is required. The assisting force is always against gravity and toward adduction (backwards). Because the assistance is required at the same time when the spine is flexed, the spine flexion and shoulder adduction forces can be mechanically coupled into a functional degree of freedom (fDOF), which is described next.

An fDOF is a strategy used by our central nervous system to control our high-DOF bodies in 3D space [16]. An fDOF implies that in certain situations two or more muscles act based on the same control signal. Thomas *et al.* have shown that during reaching tasks 94.7% of the peak-to-peak dynamic torques (i.e. excluding gravitational components) at the ankle, knee, hip, spine, shoulder and elbow are determined by one parameter, i.e. one fDOF [15]. For only the hip and spine the correlation must be even higher, such that it is possible to use the BES signals from the hips, which are already measured in the HAL, as the control signal for the exo-spine.

While the mechanism explained below has some similarities with the human spine, these have mainly been chosen in order to enable the integration of several DOF with one actuator, as well as to be able to extend when flexing. For humanoid robots several spine structures have been developed [18] [19], and similar actuation systems have been used in, e.g., snake-like robots [20]. However, these systems do not need to extend when flexing or to interact with a wearer.

2.2 Mechanics

Spine hyperextension as well as movements beyond the average human spinal range of motion (ROM), which are not absolutely necessary for heavy work, were not included in the ROM of the exo-spine. In addition, position control of the spine is not needed, since the wearer himself controls the positions of the exoskeleton, so that it is sufficient to use torque control based on the wearer's BES. This method is the same as currently used in HAL-5 for other active joints. As can be seen in the schematic diagrams in Fig. 2, the proposed structure has 5 vertebrae. Each vertebra has a small ROM, and altogether they produce the required total ROM. The links between the vertebrae constrain the movements.



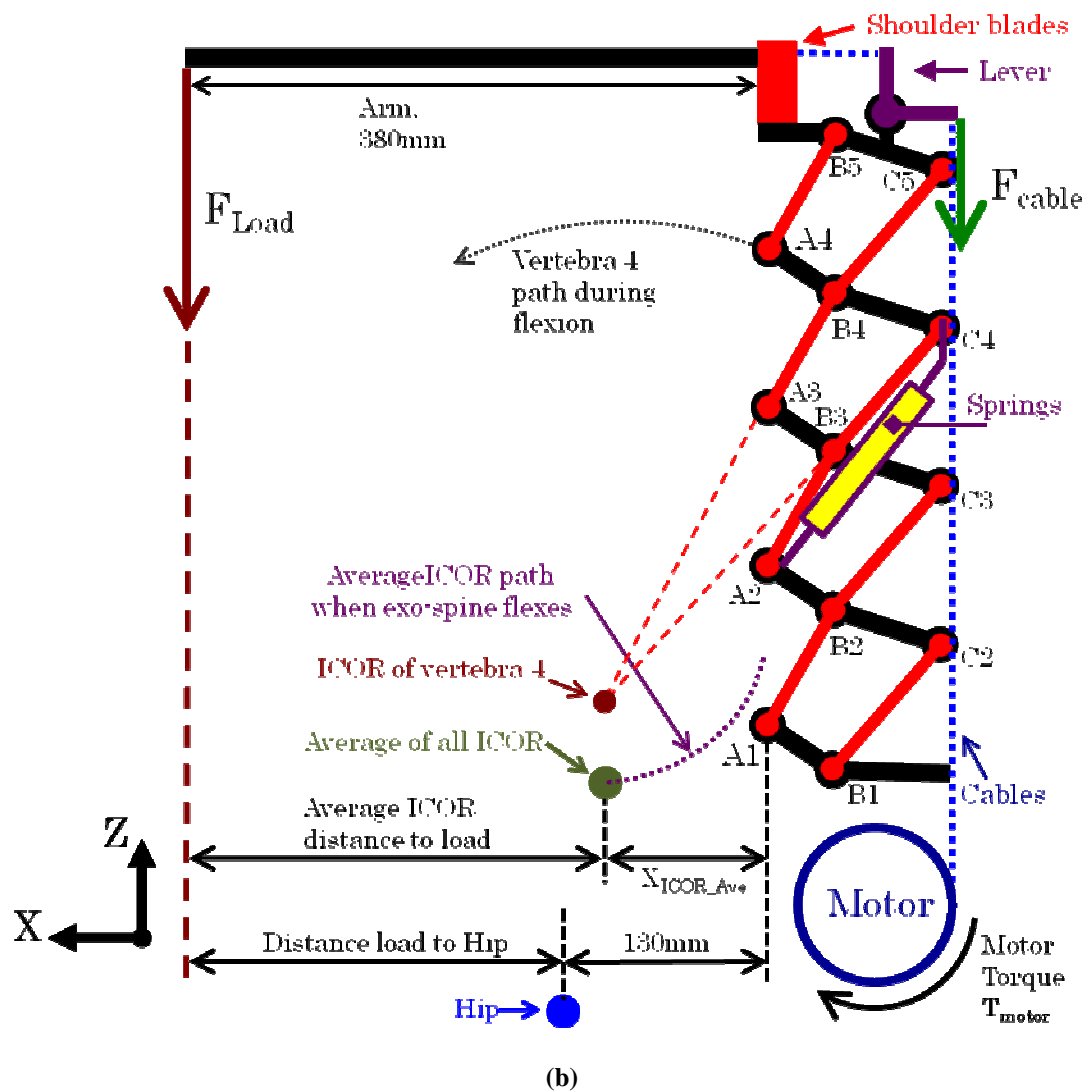


Figure 2 : Schematic diagram (side view) of the exo-spine's structure, consisting of links and vertebrae, each with three joints. Forward flexion motion is shown in (a), part (b) shows the naming of the joints according to position (A: front, B: mid, C: rear) and vertebra number. Coordinate frames at all figures can be used for comparison: X points to the front, Z to the top, and Y to the right.

Fig. 2a shows the fundamental structure and basic forward flexion motion of the exo-spine. With the vertebrae and links connected into a pantograph the whole structure flexes forward as one single DOF, and does so while extending as a whole. Fig. 2b shows the whole mechanism. The different joints here are named according to their position (A: front, B: mid, C: rear) and the number of the vertebra they belong to. When considering only forward flexion all these joints can be thought of to move as 1 DOF rotational joints. With this in mind, actuation is achieved by 2 cables (dotted line above motor in Fig. 2b) that run from a electromotor at the bottom. (In Fig. 2b they are behind each other, so that only one line is seen.) They pass all the C joints, and end at a lever at the top. (This lever is explained in the next paragraph.) When the motor provides a torque, T_{motor} , a pulling force is created in the cables, F_{cable} , that pulls the mechanism to flex upward. The upward-flexing moment created by F_{cable} balances the force produced by the load at the exoskeleton's arms, F_{load} . As for the actuation, the moment arm from the motor to the cables is 30 mm. A pre-tension spring connected to the pulleys stores some of the energy when flexing forward in order to relieve the motor. It has a constant of 25.23 N/mm and attaches through a pulley (radius 12.5 mm) to the motor output shaft to provide a pre-tension torque. Calculations of the total force balance are described in Section 2.3.

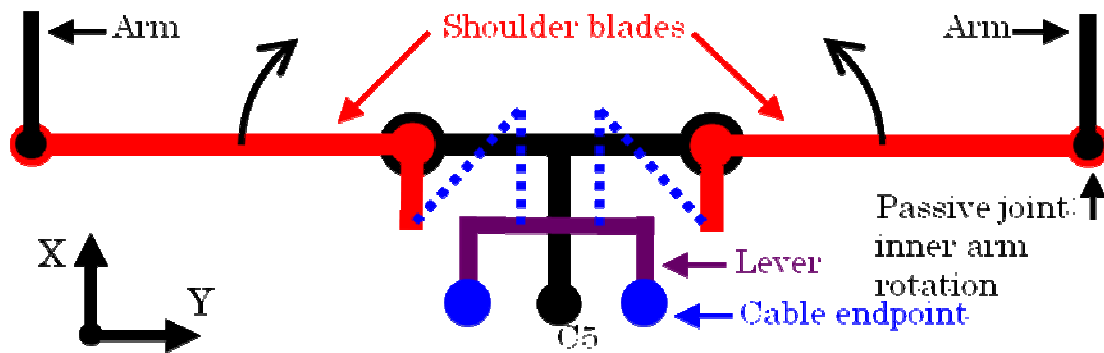


Figure 3 : Schematic diagram (top view) of the top vertebra (middle, black, vertebra 5) and the shoulder blades.

The two cables that actuate the spine are connected to a lever at the top vertebra (Fig. 2b). From this lever two other cables each support one “shoulder blade”. These shoulder blades are shown schematically in Fig. 3. They enable abduction of each shoulder. The lever’s moment arm ratio between the two sets of cables is determined such that the assisting force towards adduction of the shoulders balances that of the spine during deep bending.

To enable lateral flexion and spine rotation the mechanism’s joints have been made as follows: the front (A) joints are 1 DOF rotational joints; the mid (B) joints are 3 DOF ball joints (rod ends), and the rear (C) joints are 3 DOF ball joints with 1 translational joint. This translational joint is explained in Fig. 4b. Each link contains joints P1-P2-P3-P4 that form a parallelogram. With this, joint C is able to move sideways (as in Fig. 4c), which is normal to the view of Fig. 2b. With this motion each vertebra’s C joint can rotate around its B joint. This enables the rotation of the whole exo-spine. Lateral flexion is made possible by the rod ends at joints B and C, as shown in Fig. 4d. Each vertebra can flex sideways at these joints. These small lateral flexions of each vertebra altogether produce the total lateral flexion ROM of the exo-spine. Fig. 5 shows CAD drawings of the actual vertebrae (top) and links (bottom). The two cables that actuate the exo-spine run through the small pulleys located around each vertebra’s C joint. They are indicated in Fig. 5a by “VP” for the vertebra pulleys and “LP” for the link pulleys.

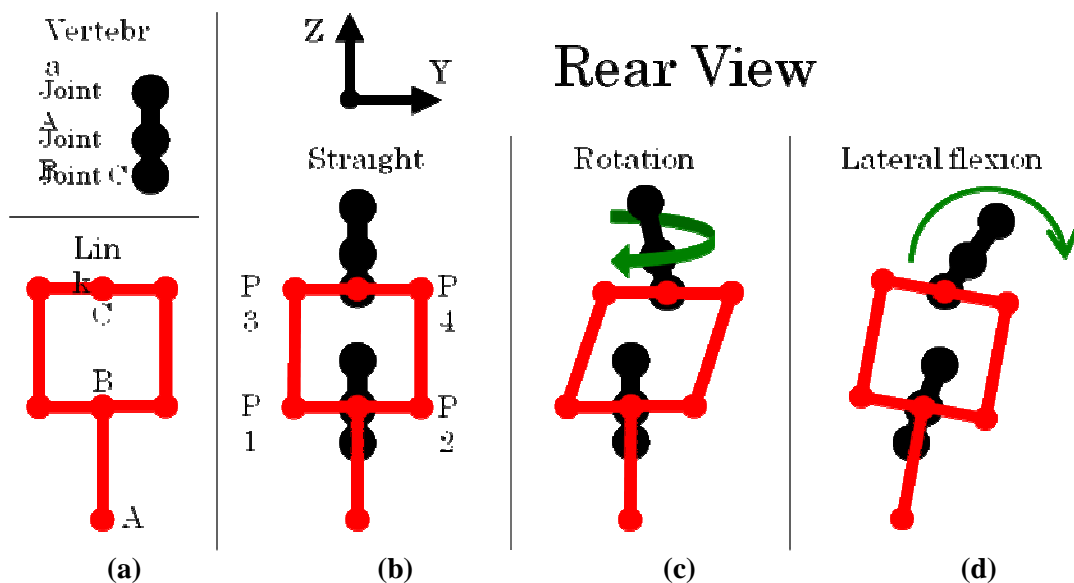


Figure 4 : Schematic diagram (rear view) of 1 link and 2 vertebrae showing their movement during rotation and lateral flexion.

Actuation of both lateral flexion and rotation is achieved by the same two cables and motor as for forward flexion. When flexing laterally to, for example, the right, the cable on the right side becomes slack, such that the left cable produces a moment back towards the neutral position. This helps balancing the load when flexing laterally. As for rotation, the changing positions of the vertebra and link pulleys cause the cables to become zigzagged, thus producing a small torque toward the neutral position.

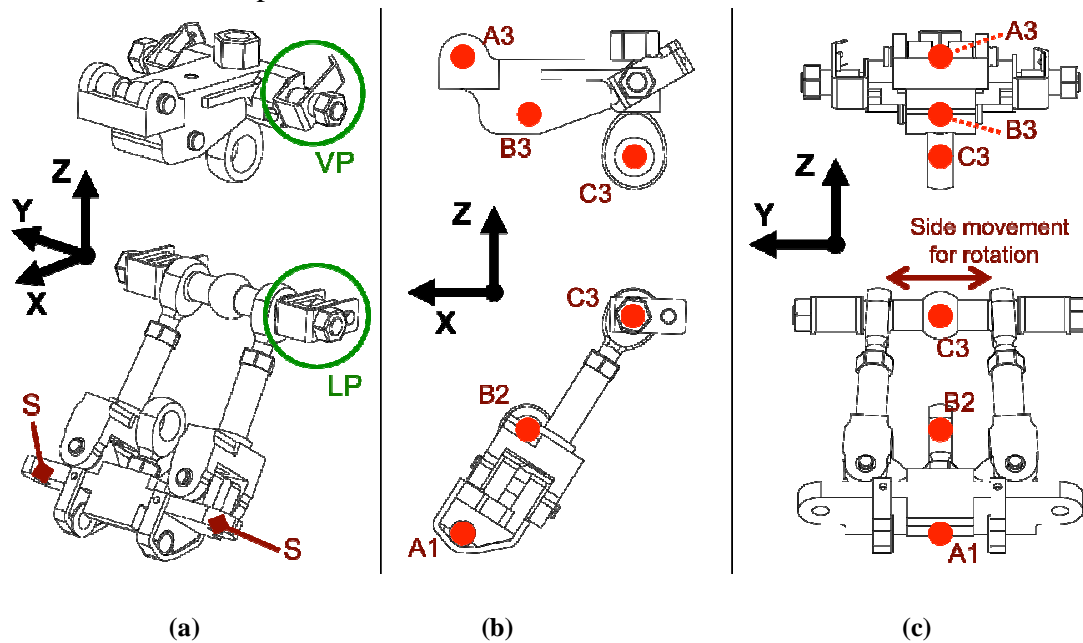


Figure 5 : CAD drawings of one vertebra (top) and one link (bottom), with (a) general view, (b) left side view, (c) front view. Joints are indicated with red dots and named as in Fig. 2b. The spring attachments are indicated in (a) by “S”, one vertebra pulley by “VP”, and one link pulley by “LP”.

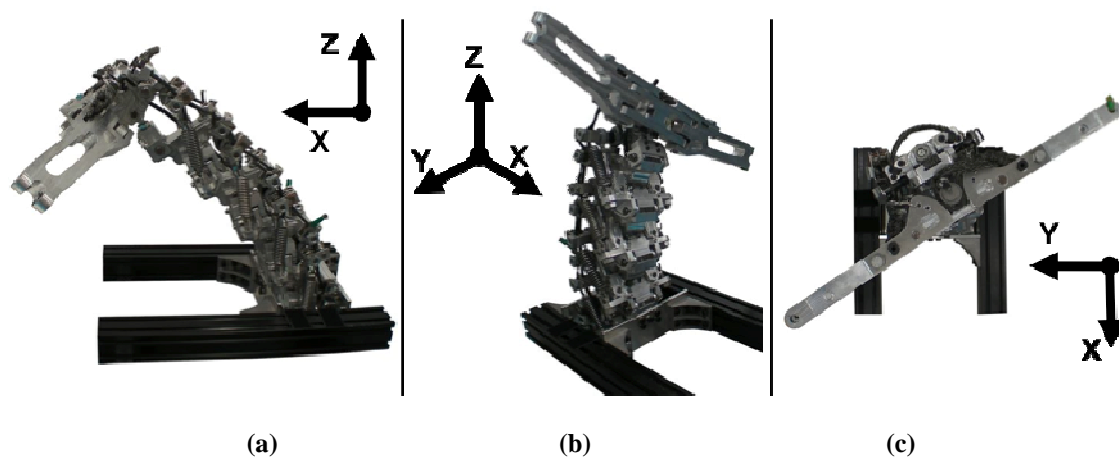


Figure 6 : Pictures of the actual prototype for (a) spine flexion and shoulder abduction, (b) lateral flexion, and (c) rotation. The black beams in the pictures were used for temporary support.

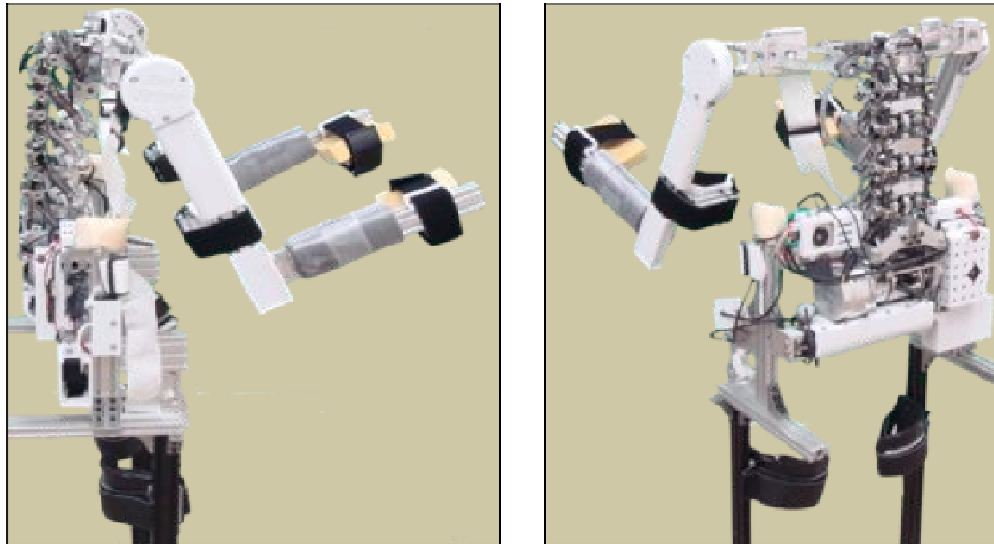


Figure 7 : Full exo-spine system with motor, electronics, and simplified legs and arms to verify its performance.

Fig. 6 shows the exo-spine prototype itself. The total height is 350 mm, spanning the upper two-thirds of the human spine. Figure 7 shows the exo-spine attached to a simplified exoskeleton for experimentation.

For stability there is one more precaution to be taken. Because the individual positions of the vertebrae are not controlled the mechanism can buckle sideways (limited to a deflection of 10 mm at the center). The exo-spine is therefore equipped with springs, 2 per link (left and right sides), shown in Fig. 2b for one link. They simultaneously balance the weight of the arms and shoulders sideways. These springs are fixed at “S” in Fig. 5a with each connecting to a short cable that passes pulley LP and is fixed next to pulley VP. Buckling is still possible, but happens only occasionally.

Furthermore, to be able to fully control the exo-spine it will be necessary to calculate the flexion moment on the spine, M_{spine} . Suppose the exo-spine would have only two vertebrae, a fixed base and one moving vertebra, then M_{spine} would be calculated as the load times the distance to the instantaneous center of rotation (ICOR) of the vertebra. The position of the ICOR can be determined as shown in Fig. 2b for vertebra 4. The ICOR of all vertebrae can then be combined into an average ICOR for the whole exo-spine, but when doing so the relative flexion speeds of all vertebrae, which change for different flexion angles, should be incorporated. The rotational energy balance per infinitesimal amount of flexion is therefore calculated and used to determine the horizontal distance (i.e. in the X-direction) of joint A1 to the average ICOR, which is X_{ICOR_Ave} (shown in Fig. 2b), as follows:

$$F_{1,2,3}(\partial\alpha_{1,2}X_1 + \partial\alpha_{2,3}X_2 + \partial\alpha_{1,3}X_3) - F_{4,5,6}(\partial\alpha_{4,5}X_{4,5,6}) \tag{1}$$

$$X_{ICOR_Ave} = (\partial\alpha_{1,2}X_1 + \partial\alpha_{2,3}X_2 + \partial\alpha_{1,3}X_3) / \partial\alpha_{1,2} \tag{2}$$

where $\partial\alpha_{ij}$ is the infinitesimal change in the angle between vertebrae i and j (with $\partial\alpha_{51}$ the change in angle between top and bottom, equal to the sum of all other $\partial\alpha_{ij}$ in (1)), and X_k is the horizontal distance between joint A1 and the ICOR of the k -th vertebra. Note that it does not matter with respect to which point X_k is defined, since the average ICOR is a fundamental property of the mechanism. For the vertical Z-position with respect to A1 a similar calculation can be made. The average ICOR moves backward and then upward as shown in Fig. 2b.

2.3 Control equations

To enable control of the motor torque based on the wearer’s BES signal, it is necessary to know the relationship between the desired total hip moment, M_{hip} , which is directly based on the wearer’s hip BES, and the required torque of the exo-spine’s motor, T_{motor} . This can be obtained by measuring the support force generated at the exoskeleton’s arms at a certain distance in front of the exo-spine’s shoulder and for a certain T_{motor} . At present there is no load estimation functionality in HAL, however, so that the load position must be assumed. In this research the position is set to 380 mm in front of, and at the same height as the top vertebra. SolidWorks simulations indicated this assumption will result in a maximum error of 6% when the load is held at extremely close or distant (stretched arm) positions. Because of the friction there is furthermore a difference in the support force between flexing up and flexing down. A setup has been prepared as shown in Fig. 8, using a force sensor connected to a horizontal rail to measure the vertical support forces (against gravity) produced by the exo-spine as it is moved up and down on a forklift to make it flex up and down. The pre-tension spring was not installed.

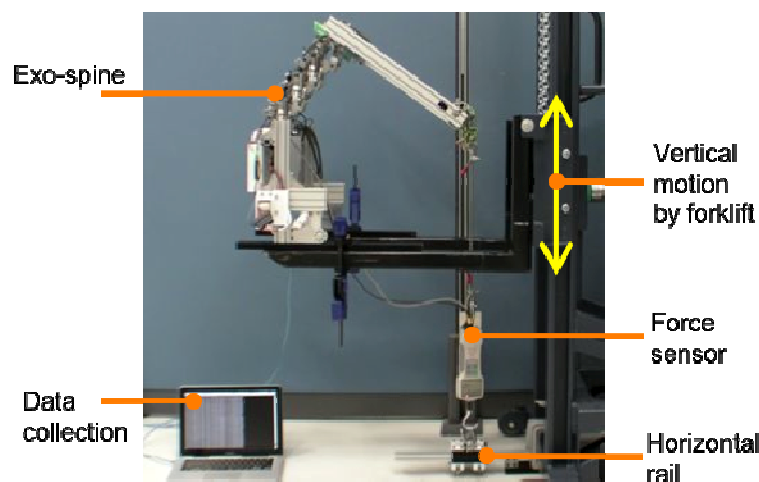


Figure 8 : Setup to measure the relationship between motor torque and supporting force.

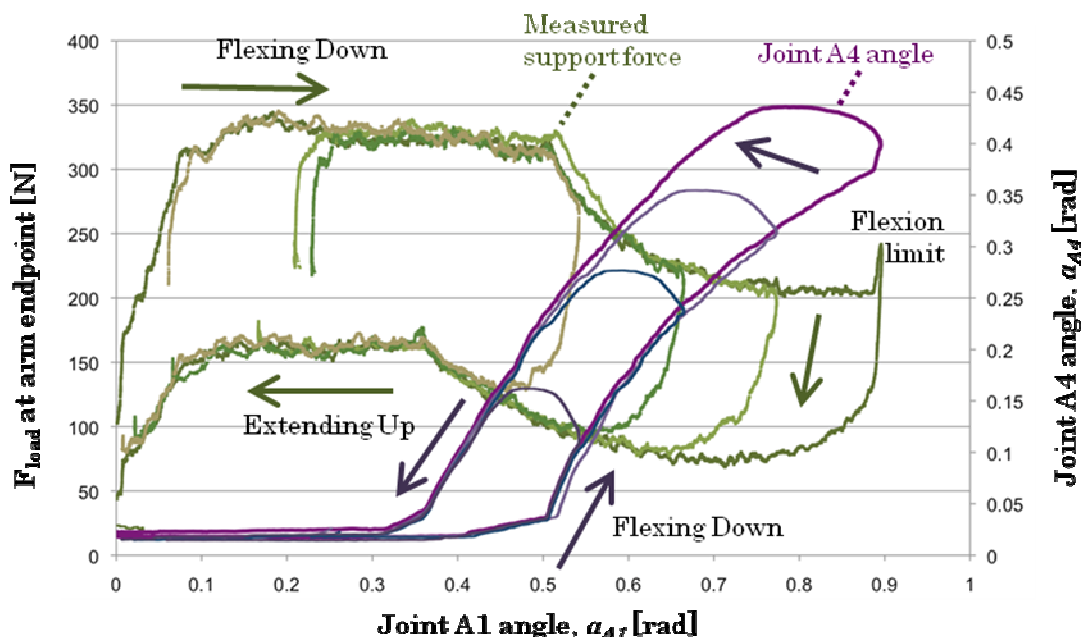


Figure 9 : Force measured at the arm endpoint (380 mm in front of the top vertebra) and the angle of joint A4, α_{A4} , versus the angle at joint A1, α_{A1} , during four measurements with a constant 14.5 Nm motor torque when moving the exo-spine down and up (as indicated by arrows).

Figure 9 shows four different down-up cycles of the measured force versus the rotation of joint A1, α_{A1} , which is a measure of the forward spine flexion (0 rad is when the exo-spine is straight). T_{motor} was 14.5 Nm. The start and end points were different for each cycle to confirm the repeatability. About halfway both flexing down and extending upward the force shows an inflection point. This is directly related to the rotation at joint A4, α_{A4} , also shown in Fig. 9, which itself is the result of the internal force balance between the links and vertebrae.

The up-down motion has been performed for a range of values of T_{motor} , and at a constant speed. The measured M_{hip} , divided by the used motor torque, are collected in Fig. 10 for the downward motions as an example (T_{motor} values are indicated in the figure). In here, M_{hip} is the product of F_{load} and the horizontal distance between the load and the intended position of the hips, 130 mm in front of A1 (see Fig 2b). Using this data the friction can be estimated by finding the common component (different for down and up) that, when subtracted from each measurement, places all measurements for, for example, the down motion onto one line. This friction component must comply with the physics of the friction [21] [22], which is assumed to be Coulomb friction and independent of speed: it can only be a function of the mechanism's configuration and internal forces. It was found to be equal to (3)-(7). In here, $F_{DWN,A1}$ is the component of the friction that depends on α_{A1} during downward flexion. This is similar for $F_{DWN,A4}$, $F_{UP,A1}$, and $F_{UP,A4}$, with UP indicating upward flexion. Parameter $F_{UP,pulley}$ is the friction component that depends on the torque at the pulleys that drive the two cables, T_{pulley} , which is the sum of T_{motor} and the torque produced by the pre-tension spring, T_{spring} , as in (8).

$$\begin{cases} F_{DWN,A1} = 0 & (\alpha_{A1} < 0.192) \\ F_{DWN,A1} = 99(\alpha_{A1} - 0.192) & (0.192 \leq \alpha_{A1} < 0.66) \\ F_{DWN,A1} = 99(\alpha_{A1} - 0.192) - 30(\alpha_{A1} - 0.66) & (\alpha_{A1} > 0.66) \end{cases} \quad (3)$$

$$F_{DWN,A4} = -106(\alpha_{A4} - 0.064)^{0.66} \quad (\alpha_{A4} > 0.064) \quad (4)$$

$$\begin{cases} F_{UP,A1} = 4.5 + 11\alpha_{A1} & (\alpha_{A1} \leq 0.74) \\ F_{UP,A1} = 4.5 + 11\alpha_{A1} - 6(\alpha_{A1} - 0.74) & (\alpha_{A1} > 0.74) \end{cases} \quad (5)$$

$$F_{UP,A4} = -23(\alpha_{A4} - 0.05)^{0.43} \quad (\alpha_{A4} > 0.05) \quad (6)$$

$$F_{UP,pulley} = -0.7(12 - T_{pulley}) \quad (T_{pulley} < 12) \quad (7)$$

$$T_{pulley} = T_{motor} + T_{spring} \quad (8)$$

In addition, the motor itself has an estimated friction of 2 Nm.

The lines containing all data points after deduction of the friction are shown in Fig. 11 for downward flexion. The lines have been separated into three parts in order to obtain a polynomial fitting. The resulting equations give the torque ratio, TR , which is used to determine the motor torque from the desired M_{hip} . They are as follows for downward motion.

$$\begin{cases} TR = 5.585 & (\alpha_{A1} < 0.084) \\ TR = 6973\alpha_{A1}^4 - 4825\alpha_{A1}^3 + 1114\alpha_{A1}^2 - 88.8\alpha_{A1} + 7.70 & (0.084 \leq \alpha_{A1} < 0.266) \\ TR = 267\alpha_{A1}^4 - 464\alpha_{A1}^3 + 276\alpha_{A1}^2 - 66.3\alpha_{A1} + 12.5 & (0.266 \leq \alpha_{A1} < 0.66) \\ TR = -0.47\alpha_{A1}^2 - 0.494\alpha_{A1} + 6.58 & (\alpha_{A1} > 0.66) \end{cases} \quad (9)$$

For upward motion they are

$$\begin{cases} TR = 3.183 & (\alpha_{A1} < 0.075) \\ TR = -697\alpha_{A1}^3 + 227\alpha_{A1}^2 - 14.2\alpha_{A1} + 3.27 & (0.075 \leq \alpha_{A1} < 0.187) \\ TR = -58.3\alpha_{A1}^4 - 206\alpha_{A1}^3 + 186\alpha_{A1}^2 - 43.3\alpha_{A1} + 6.97 & (0.187 \leq \alpha_{A1} < 0.383) \\ TR = -68.6\alpha_{A1}^4 + 169\alpha_{A1}^3 - 144\alpha_{A1}^2 + 45.3\alpha_{A1} + 0.621 & (\alpha_{A1} > 0.383) \end{cases} \quad (10)$$

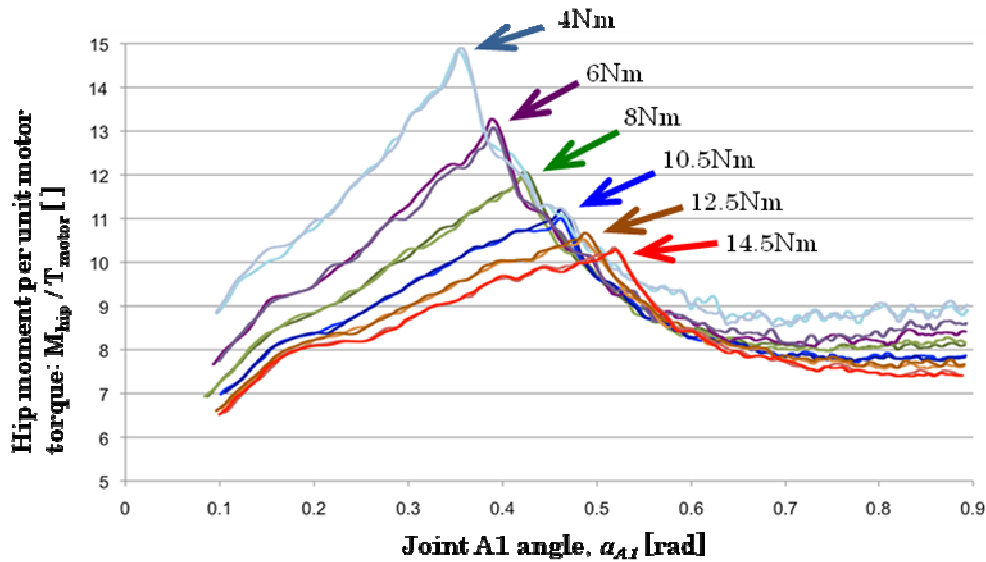


Figure 10 : Measured hip moment per unit of motor torque for downward flexion (twice per torque value).

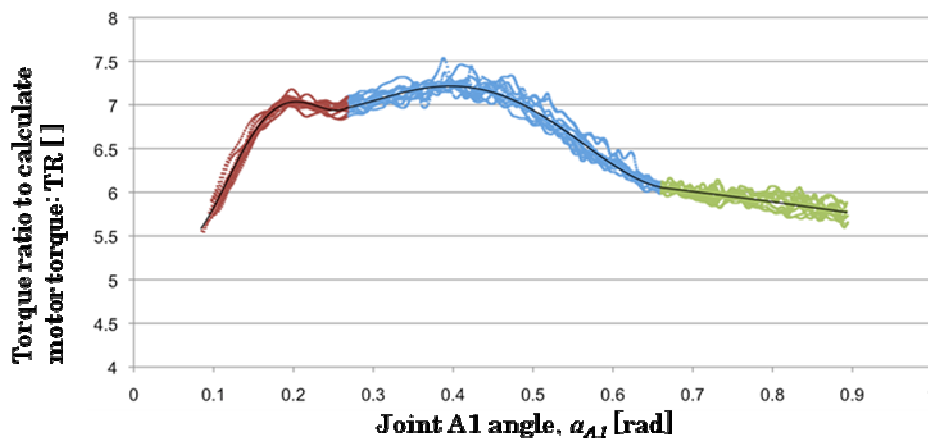


Figure 11 : Final measurement data after subtraction of the friction for downward flexion. Polynomial fittings for the three colored areas are shown in (9).

For low α_{A1} angles TR is constant. If not, TR would decrease further, leading to high motor torques. Finally, T_{motor} is calculated as follows when flexing down:

$$T_{motor} = -2 + (M_{hip} - F_{DWN,A1} - F_{DWN,A4}) / TR - T_{spring} \quad (11)$$

and when flexing up

$$T_{motor} = 2 + (M_{hip} - F_{UP,A1} - F_{UP,A4} - F_{UP,pulley}) / TR - T_{spring} \quad (12)$$

The controller chooses to use the down or up equations based on the intention of the wearer, as is shown in Fig. 12. When not moving the controller switches to the down state to save energy, essentially using the friction as extra support. It switches to up when the spine is moving up or when the wearer increases his M_{hip} beyond a threshold. This threshold is a leaky bucket counter combined with a 1s hold function to give the wearer time to actually move up. When switching from down to up the torque increase is spread over 1s to dampen any shock to the wearer.

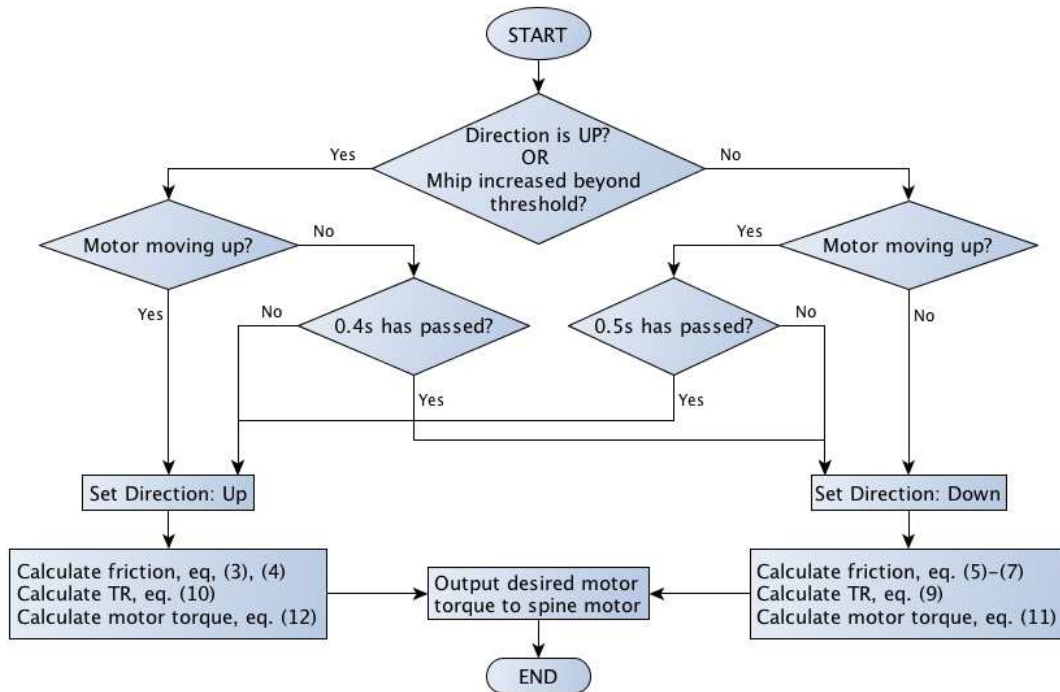


Figure 12 : Block diagram of the direction decision algorithm that chooses between the down and up state. Time constants were determined experimentally.

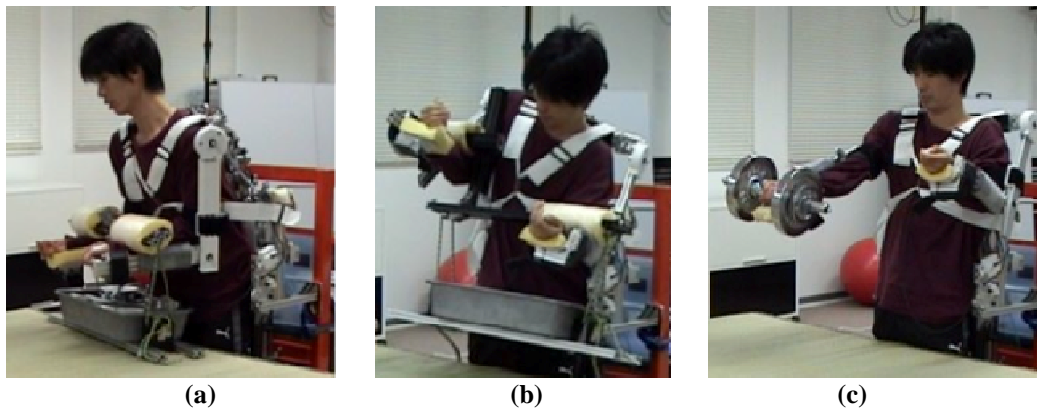


Figure 13 : Experiment snapshots for (a) lifting with rotation, (basic lifting is similar but without spinal rotation), (b) lifting with lateral flexion, (c) one arm lifting.

Table 1: Shoulder and elbow angles during experiments.

Experiment	Shoulder angle Left / Right	Elbow angle Left / Right
1) Basic lifting, Fig. 13a	0.54rad / 0.54rad	1.54rad / 1.54rad
2) Lifting with rotation, Fig. 13a	0.54rad / 0.54rad	1.54rad / 1.54rad
3) Lifting with lateral flexion, Fig. 13b	0.54rad / 1.08rad	1.54rad / 1.16rad
4) One arm lifting, Fig. 13c	0.54rad / 1.35rad	1.54rad / 0.13rad

RESULTS

First of all the ROM of each single DOF was measured. This will be important for evaluating the experiment results. The maximum range for each single DOF is 44deg flexion (0.77rad, equal to $\alpha_{A1} = 0.95$ rad), 33deg (0.58rad) lateral flexion, 32deg (0.56rad) rotation and 64 mm of forward abduction at the endpoints of the shoulder blades.

3.1 Lifting experiments and results

The exo-spine was attached to simplified legs and arms (Fig. 7) and four different lifting experiments have been performed to confirm the performance of the exo-spine. While all four are, mechanically, fundamental movements, they are also based on specific nursing actions [4] [23] [24]. Although spine motion is advised against for nursing tasks, it could become allowed when an exoskeleton provides most of the support. The experiments are:

1 Basic lifting

Lifting up and setting down using only forward spine flexion, while lifting loads of 20, 30, and 40 kg placed on the lower arms. Particularly used in patient transfer tasks, and when helping a patient to stand up.

2 Lifting with rotation

Lifting up, rotating with load from left to right (or vice-versa) as far as possible, as in Fig. 13a. Loads of 20, 30, and 40 kg are used. For nursing this motion is used during patient repositioning tasks.

3 Lifting with lateral flexion

The load in the experiment was asymmetric, such that one arm has to be higher in order to hold the load horizontal (Fig. 13b). Actions were: lifting up, going down while bringing load horizontal, setting down. Loads are 20, 30, and 40 kg. For nursing this motion is used when one arm is at a higher position than the other, such as when lifting up someone's legs from the floor onto the bed.

4 One arm lifting

Lifting up with one stretched arm (most extreme reaching case), and setting down, as in Fig. 13c. Loads of 10 and 15 kg were used (additional wrist support was provided). Such a motion is used in practice when reaching over the bed to lift up a part of the patient.

The angles of the shoulders and elbows during the experiments are listed in Table 1. There were several safety precautions including torque limitations (maximum T_{motor} : 25 Nm, maximum M_{hip} : 120 Nm), and the placement of the loads below the wearer's arms using a beam with ropes, as in Fig. 15a and b. The subject was an adult male (1.72m, 52 kg). He was fixed to the system using straps at the legs and arms and bands that cross the chest, similar to full body exoskeletons. To measure M_{hip} , which is an extension torque during lifting, the BES of each leg's hip extensor, gluteus maximus, was measured.

Figures 14 and 15 show typical examples of experiment results for two lifting cycles each of 20 kg basic lifting (14a), 30 kg lifting with rotation (14b), 40 kg lifting with lateral flexion (15a), and 15 kg one arm lifting (15b). At the top are shown the angles of the line connecting the glenohumeral joints of the exo-spine, with β_{Sh} indicating rotation (as viewed from above, projected onto the horizontal XY plane), and γ_{Sh} indicating lateral flexion (the angle with the horizontal XY plane), measured using motion capture. Directly below are the angles of the

exo-spine's joint A1 (α_{A1}), joint A4 (α_{A4}) and right shoulder blade ($\alpha_{ShBl,R}$). Angles are zero when the exo-spine is straight up. The highest possible value for $\alpha_{ShBl,R}$ is 0.47 rad at 64 mm abduction. Next are shown M_{hip} , T_{motor} , and the motor controller's state for the direction, up or down, with grey areas indicating up. The motor torque becomes negative at times to compensate for the motor friction and, the spring pre-tension.

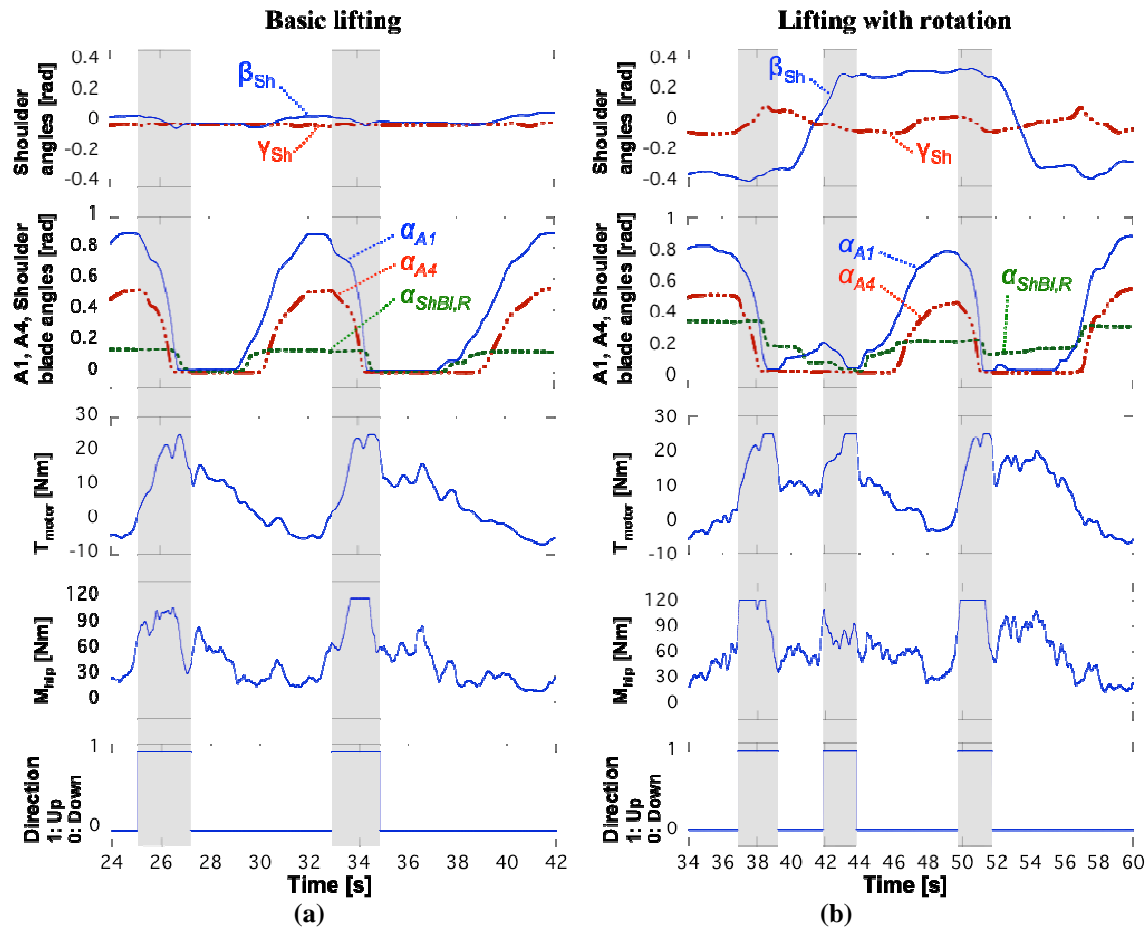


Figure 14 : Experiment results showing two lifting cycles for (a) experiment 1 (basic lifting, 20 kg), and (b) experiment 2 (lifting with rotation, 30 kg). Shown are, from the top, the angles of the exo-spine's shoulder girdle: rotation β_{Sh} and lateral flexion γ_{Sh} , the exo-spine's joint angles A1 (α_{A1}), A4 (α_{A4}) and right shoulder blade ($\alpha_{ShBl,R}$), motor torque T_{motor} , hip moment, M_{hip} , commanded by the wearer's BES, and the controller's direction status, with 1 indicating up (grey areas).

DISCUSSION

In the lifting experiment described above the subject was able to lift up all loads successfully. Each time the controller noted the increase in muscle activity of the subject, and thus in M_{hip} , and switched to the up state, after which the subject could lift up the load within 1s to 4 s time. Occasionally, such as in Fig. 14b at 42s, it was necessary to extend the exo-spine up again after it had flexed down more than intended. In such cases the subject increased his muscle activity again in order to re-activate the up state. In a few other cases, such as between 37s and 42s in Fig. 15a, the subject had to brake a flexion motion that was too fast by re-activating the up state. Given the quick increase of M_{hip} following the flexion motion it seems this was an automatic muscle reflex of the hip muscles that may require a further fine-tuning of the controller. In addition it can be seen that especially when lifting heavy loads the maximum M_{hip} and T_{motor} were reached often during lifting up. This limitation will be further relaxed, however, with subsequent experimentation. Overall the exo-spine was successful in enabling the subject to lift

up heavy loads while moving his spine and shoulders. With a fixed back none of the movements would have been possible. That the exo-spine indeed supported the lifting can be verified from the motor torque, which has been shown in section 2.3 to provide support against gravity forces.

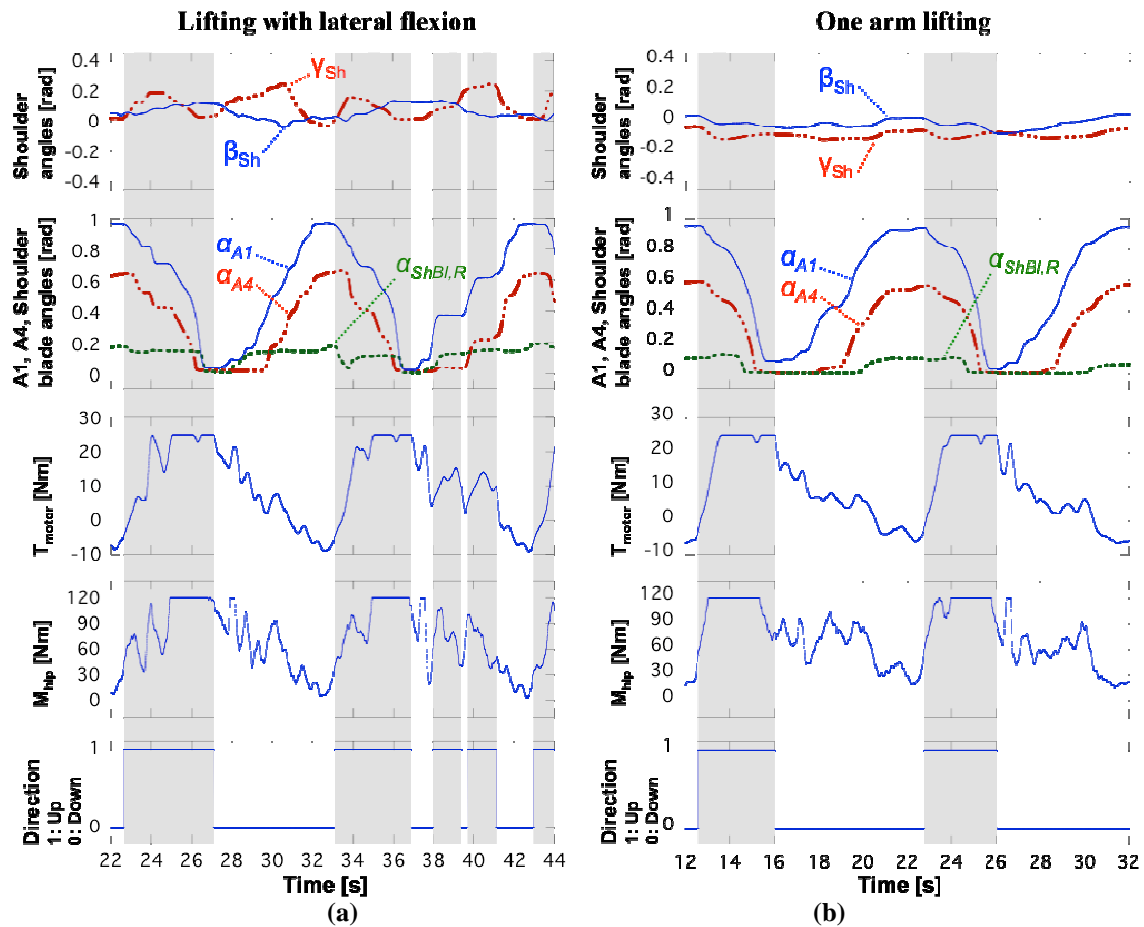


Figure 15 : Experiment results showing two lifting cycles for (a) experiment 3 (lifting with lateral flexion, 40 kg), and (b) experiment 4 (one arm lifting, 15 kg). The parameters shown are the same as in Fig. 16.

As for the ROM of the exo-spine, when comparing it to the human spinal ROM it can be seen that only the flexion ROM is about 10deg less [25]. Although it could be extended by adding a vertebra and a link, it would not be advisable as the human spine becomes weaker when fully flexed [26]. When comparing the maximum ROM of each DOF with the ROM used in the experiment, it can be concluded that while the forward flexion ROM was used completely, there was still movability left in the other DOF.

In the case of rotation (Fig. 14b) about 2/3 of the total ROM was used. Here, the main limitations were the allowable space for the load as well as the torque from the exo-spine pushing the wearer back toward the neutral position, especially with higher loads. Similarly, the assisting torque during lateral flexion was the reason that less than 50% of the lateral flexion ROM was used. With more load on the lower arm this motion actually becomes easier, but further experiments using additional active DOF (at the hips, shoulders, etc) would be needed to confirm whether more motion is actually required. Lastly, shoulder abduction was used mostly in combination with rotation and for about 2/3. However, it will only become really required when the whole trunk flexes forward for deep bending motions.

With the increases in DOF there is, however, also a substantial amount of friction in the system

due to the use of rod ends. Although this results in energy losses when lifting something up, it actually reduces the amount of motor torque when standing still or moving down. Moreover, as can be seen in the experiment results, even when continuously moving up and down the percentage of time the controller spends in the up state is still quite low. With the controller also in the down state when the exo-spine is not moving, it may be concluded that the friction actually helps to save energy.

CONCLUSION

This paper addressed the importance of the current flexibility limitations in full body exoskeletons, particularly for applications in the health care field. A solution called exo-spine was proposed in order to fulfill the purpose of this paper: to enable 3 DOF spinal and 2 DOF shoulder girdle motion with augmentation for lifting in the front. The 5 DOF flexibility of the mechanism was confirmed using ROM measurements as well as experiments in which the exo-spine enabled a subject to lift up weights of up to 40 kg on his lower arms using all DOF of his spine while performing motions similar to those used in nursing techniques. From this experiment we could therefore confirm the performance of the exo-spine and thus its applicability for full body exoskeletons in health care applications.

The exo-spine will first be extended into a full body HAL robot suit in order to test it fully in a health care setting. At this time extensive experimentation will be needed to cover a large range of possible lifting situations in order to verify the full effectiveness. Eventually, health care workers wearing an exoskeleton will be able to, for example, reach behind a patient while leaning over his bed, while in other fields such as rescue operations [27] wearers will be able to find a proper lifting posture when standing on the rubble.

Acknowledgements

This work was supported in part by the Global COE Program on “Cybernetics: fusion of human, machine, and information systems”, as well as the “Funding Program for World-Leading Innovative R&D on Science and Technology (FIRST Program),” initiated by the Council for Science and Technology Policy (CSTP).

REFERENCES

- [1] Prabakaran L, and Vishalini M, *Der Pharmacia Sinica*, **2010**, 1 (1): 147-165
- [2] K. Saroha, P. Mathur, S. Verma, N. Syan and A. Kumar, *Der Pharmacia Sinica*, **2010**, 1 (1): 179-187
- [3] J.M. Tullar, S. Brewer, B.C. Amick, E. Irvin, Q. Mahood, L.A. Pompeii, A.N. Wang, D. Van Eerd, D. Gimeno, and B. Evanoff, *J. Occup Rehabil.*, Epub, **2010**
- [4] A. Nelson, and A.S. Baptiste, *Orthop Nurs.*, **2006**, 25, pp. 366–79
- [5] R.E.A. Van Emmerik, M.T. Rosenstein, W.J. McDermott, and J. Hamill, *Nonlinear Dynamical Approaches to Human Movement*, Journal of Applied Biomechanics, **2004**, vol. 20
- [6] Y. Sankai, *International Joint Conference SICE-ICCAS*, Busan (Korea), **2006**, pp. 27–28
- [7] K. Yamamoto, K. Hyodo, M. Ishi and T. Matsuo, *JSME Int. J., Series C: Mechanical Systems, Machine Elements and Manufacturing*, **2002**, vol 45, n. 3, pp. 703-711
- [8] J.C. Perry, J. Rosen, and S. Burns, *Mechatronics, IEEE/ASME Transactions on*, **2007**, vol.12, no.4, pp. 408-417
- [9] C. Hirsh and T. Karloski, *Ninth Annual Freshman Conference*, University of Pittsburgh, **2009**
- [10] M.S. Liszka, M.S. thesis, Univ. of Maryland, **2006**

- [11] S. Toyama, and G. Yamamoto, *Proc. IEEE/RSJ International Conference on Intelligent Robots and Systems*, **2009**, pp.5801-5806
- [12] A. Schiele, and F.C.T. Van der Helm, *IEEE Trans Neural Systems and Rehabilitation Eng*, **2006**, 14(4), pp. 456-69
- [13] M. Folgheraiter, B. Bongardt, S. Schmidt, J. De Gea, J. Albiez and F. Kirchner, *Proc. Interfacing the Human and the Robot Workshop, ICRA*, **2009**, Kobe, Japan
- [14] S.R. Taal and Y. Sankai, *Proc. Int'l Conference on Robotics and Automation*, **2011**, Shanghai, China
- [15] J. Rosen, J.C. Perry, N. Manning, S. Burns and B. Hannaford, *Proc. 12th Intl. Conf. on Advanced Robotics, ICAR '05*, **2005**, pp. 532-539
- [16] M.L. Latash, J.P. Scholz and G. Schöner, *Motor Control*, **2007**, vol 11, pp. 275-307
- [17] J.S. Thomas, D.M. Corcos and Z. Hasan, *Journal of Neurophysiology*, **2005**, vol 93, pp. 352-364
- [18] I. Mizuuchi, S. Yoshiada, M. Inaba, and H. Inoue, *Advanced Robotics*, **2003**, 17(2), pp. 179-196
- [19] L. Roos, F. Guenter, A. Guignard, and A.G. Billard, *Proc. Biomedical Robotics and Biomechatronics*, **2006**, pp.329-334
- [20] S. Hirose, and H. Yamada, *Robotics & Automation Magazine, IEEE* , **2009**, vol.16, no.1, pp.88-98
- [21] A. K. Kaviti, O. Prakash and P. Vishwanath, *Advances in Applied Science Research*, 2011, 2 (5): 279-289
- [22] V.P. Rathod and S. K. Asha, *Advances in Applied Science Research*, **2011**, 2 (4):102-109
- [23] B. Schibye, A. Faber Hansen, C.T. Hye-Knudsen, M. Essendrop, M. Bocher, J. Skotte, *App Ergonom*, **2003**, 34, pp. 115 – 123
- [24] M. Shogenji, K. Izumi, A. Seo, and K. Inoue, *J. of the Tsuruma Health Science Society*, **2007**, Vol.31(2), p.p.57~69
- [25] N. Berryman Reese and W.D. Bandy, *Joint Range of Motion and Muscle Length Testing*, Elsevier Health Sciences, **2009**, pp. 476-477
- [26] J.L. Gunning, J.P Callaghan, and S.M. McGill, *Clinical Biomechanics*, **2001**, 16:471– 80
- [27] J. Punithavathi , S.Tamilenthi and Baskaran, *Advances in Applied Science Research*, **2011**, 2 (2): 437-449